Reprinted From "Advances in Biomagnetism", S.J. Williamson, M.Hoke, G. Stroink, and M. Kotani, Eds., (Plenum, New York), pp.1-18 (1989) with kind permission

BIOMAGNETIC SOURCES AND THEIR MODELS

John P. Wikswo

Living State Physics Group
Department of Physics and Astronomy
Vanderbilt University
Nashville, TN 37235, U.S.A.

INTRODUCTION

Over the past twenty-five years, the study of biomagnetic phenomena has evolved into an interdisciplinary research effort involving individuals whose primary training has most often been in either biology, engineering, medicine, physics, or psychology. The goal of this tutorial is to present to a similarly eclectic audience the essential physics and electrophysiology required to describe the biological sources of magnetic fields, the spatial variation of these fields, and how the sources and their fields can be modeled mathematically. Introductory physics courses tend to concentrate on simple systems such as isolated electric charges in vacuum, currents flowing in circular coils, and circuits with discrete batteries, wires, and resistors. Introductory biology courses seldom address bioelectric phenomena in detail. As a result, many of us enter biomagnetism with an intuition that is ill-prepared to describe how biological cells produce currents that flow throughout an inhomogeneous body that has a complicated geometry. It is even harder to understand the spatial variation and information content of the magnetic fields associated with these currents. In complex systems such as the human heart or brain, the simple equations presented in an introductory physics course must be written in a more general form, usually involving vector or tensor calculus. Rigorous and quantitative treatment of this material can be found in several chapters in the volume edited by Williamson *et al.* (1983), in the text by Hobbie (1988), and in the review by Wikswo *et al.* (1979). Kuffler *et al.* (1984) and Macfarlane and Lawrie (1989) provide comprehensive treatments of neurophysiology and cardiac electrophysiology, respectively. In this tutorial, I will concentrate on presenting a more qualitative, pictorial approach to the subject than do any of these references. I hope that I will describe the concepts in a manner that will allow someone whose background does not span all of physics, mathematics, and biology to develop an appreciation for the interdisciplinary subtleties of the subject without the distraction of numerous equations or extensive physiological descriptions. Because of space limitations, I will not discuss how magnetic materials, either of biological origin or from contamination, can produce magnetic fields.

Since, out of necessity, this tutorial can provide only a cursory view of the subject, two messages should be emphasized at the outset: the physiological and bioelectric phenomena at play in biomagnetism are exquisitely complicated, and the physical laws that ultimately describe them are elegant in their simplicity and generality. We now will proceed to show how these physical laws can describe biomagnetic phenomena, and in doing so will attempt to develop our own intuitive grasp of the subject.

Advances in Biomagnetism
Edited by S.J. Williamson *et al.*
Plenum Press, New York

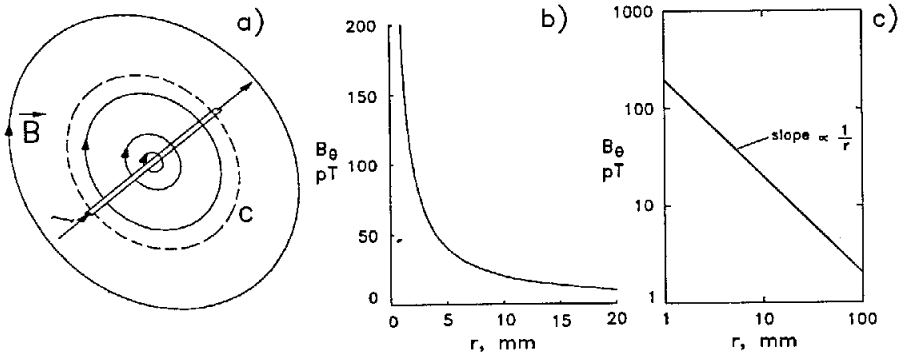

Figure 1. a) The magnetic field $\vec{B}$ produced by a current I flowing in a long, straight wire. b) Linear and c) log-log plots of the strength of the magnetic field (B_θ) encircling a wire that is carrying a 1 μA current.

SOURCES OF MAGNETIC FIELDS

As a first step toward understanding biomagnetic fields, it is useful to consider the magnetic field produced by a long wire carrying a current I. The magnetic field $\vec{B}$ from this current encircles the wire, as shown in Figure 1a. Since a magnetic field has both magnitude and direction, it is a vector quantity, which we so identify by placing an arrow above the symbol, as in $\vec{B}$. The direction (or sign) of the magnetic field encircling the wire must be chosen by mathematical convention, since the cylindrical symmetry of the problem does not provide a distinction between clockwise or counterclockwise field lines. By the right hand rule, if the extended thumb of the right hand is placed along the wire with the thumb pointing in the direction of the flow of current, the direction of the field is defined by the fingers as they wrap around the wire. The strength of the magnetic field is easily determined by Ampere's law, which, in the simple form that is applicable to our cylindrically-symmetric problem, states that the magnetic field along the closed curve c (shown in Fig. 1a by the broken circle) times the length of c is equal to a fundamental constant μ_o (the magnetic permeability of free space) times the net current threading c. Because c is threaded only by the wire, the net current is I. Ampere's law can be rearranged to yield an expression for the component of the magnetic field that is tangential to c, i.e. B_θ, at a distance r from the wire:

$$B_\theta(r) = \frac{\mu_o I}{2\pi r}, \tag{1}$$

where μ_o equals $4\pi \times 10^{-7}$ tesla-meter/ampere. In SI units, the magnetic field strength is measured in tesla. The proportionality of B_θ to $1/r$ is shown by the hyperbola in Fig. 1b and the line of slope -1 in the log-log plot in Fig. 1c. In these graphs, I is assumed to be a biologically-realistic current of 1 microampere (μA), which produces a 20 picotesla (10^{-12} T = 1 pT) magnetic field 10 mm from the wire. This field strength, less than one millionth of the 5×10^{-5} T magnetic field of the earth, would best be measured with a Superconducting QUantum Interference Device (SQUID) magnetometer.

If we take the wire in the previous example and bend it into the circle shown in Fig. 2a, the magnetic field is strengthened along the axis of the circle and is reduced outside the loop. As a result, the vertical component of the field at a distance z along the axis of a loop of radius a is given by a somewhat more complicated equation

$$B_z(z) = \frac{\mu_o I a^2}{2(a^2 + z^2)^{3/2}}. \tag{2}$$

If the loop is small in size, the field at the center of the loop is stronger than for a larger loop carrying equal current, but falls off more quickly close to the loop, as shown in Fig. 2b.

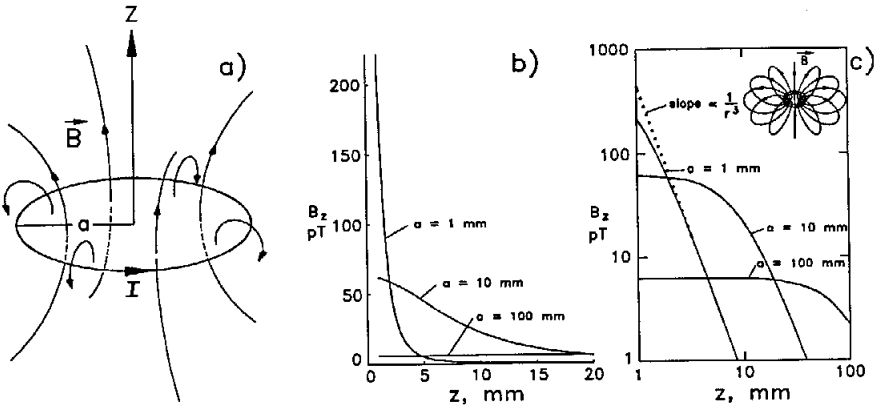

Figure 2. a) The magnetic field $\vec{B}$ produced by a current I flowing in a loop of wire of radius a. b) Linear and c) log-log plots of the strength of the magnetic field B_z along the axis of the loop, which is carrying a 1 μA current, for loops of three different radii. The inset in c) shows the dipolar magnetic field of a small current loop.

Figure 2c and Eq. (2) show that when the distance from the loop is much larger than the radius, the magnetic field falls off as $1/z^3$, independent of the size of the loop. In this far-field case, the spatial variation of the magnetic field has the pattern shown in the inset of Fig. 2c. The field is axisymmetric, comes out of the upper side of the loop, and reenters on the lower side, just as if the loop had a north pole immediately above it and a south pole immediately below. It is important to note that since isolated magnetic poles (monopoles) have not yet been found to exist, magnetic field lines must form closed curves that neither start nor stop, and hence the current loop does not really have two magnetic poles. Even so, it is useful to describe the current loop as if it were a magnetic "dipole," and hence its field pattern in Fig. 2c is "dipolar." The strength of the magnetic field is proportional to the product of the current I and the area of the loop πa^2, and this product is termed the "moment" (or strength) of the magnetic dipole.

We must now examine the sources of current that produce the magnetic field. In the simple circuit in Fig. 3a, the voltage, V, current, I, and resistance, R, obey Ohm's law, $V = IR$. If we write this as $I = V/R$, we see that for a fixed voltage, the current that flows in the circuit is inversely proportional to the resistance. As with the example in Fig. 3a, an introductory physics class is most likely to discuss magnetic fields that are produced by currents flowing in circular loops of wire. The batteries are usually kept far away from, rather than as an integral part of, the coil that produces the magnetic field. For biological systems, it would be more realistic to have both the battery, which serves as the voltage source, and the resistor, which limits the current, as integral parts of the coil, as in Fig. 3b. This figure also emphasizes the fact that the magnetic field is produced not only by the Ohmic (passive) current flowing through the wire and the resistor, but also by the electrochemically- or metabolically-driven (active) currents within the battery. Since discrete wires are seldom found in biological systems, the situation in Fig. 3c is an even better example, since the battery is placed on the surface of a container of electrically-conductive fluid such as saline, so that the current I flowing out of the positive electrode next to the resistor is dispersed into a current density $\vec{J}$ that flows throughout the saline and then returns to the negative electrode next to the battery. A current dipole is a mathematical idealization of a source for which the current flows out at one location and returns at another location that is an infinitesimal distance away. When viewed from far away, our current source looks like a current dipole whose moment q equals I times the electrode separation. If this current dipole were placed deep in a large volume of saline, its electric field would be proportional to q/r^3, where r is the distance between the dipole and the point where the field is measured. As

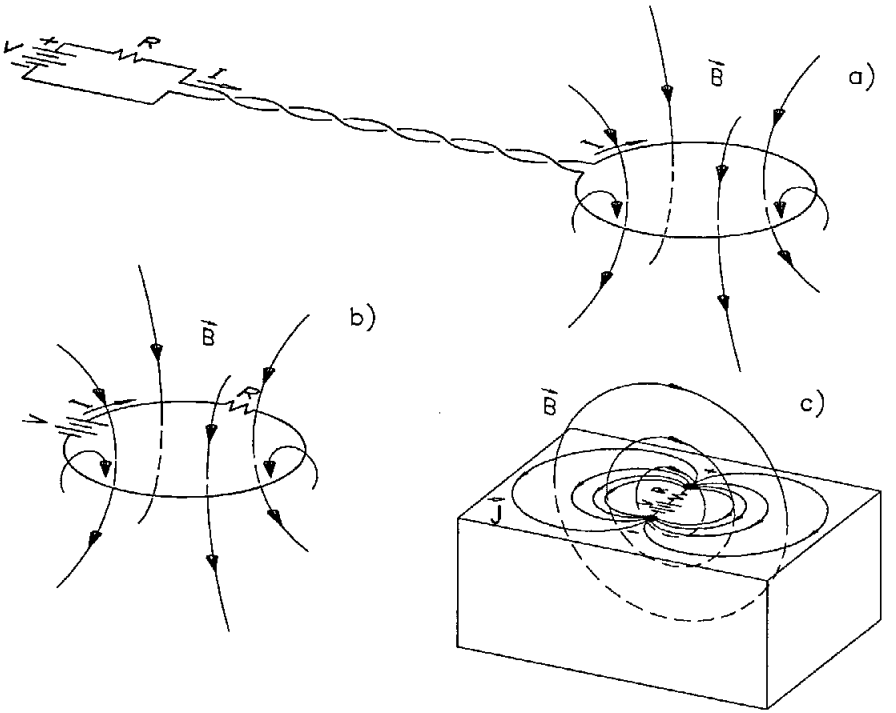

Figure 3. a) A loop of wire and its magnetic field $\vec{B}$, when the battery is far away. It follows from Ampere's law that the magnetic field from the leads connecting the battery to the loop is negligible because the leads are tightly twisted. b) A loop of wire that contains a voltage source and a current-limiting resistor. c) The current and magnetic field distributions from a current source located on the surface of a conducting bath of saline. The source can be thought of as a current dipole whose moment (i.e. strength) is the product of the spacing between the positive and negative electrodes times the current passing between them.

shown in the figure, a magnetic field encircles the *primary* current flowing within the current source. The magnetic field from this current dipole would be proportional to q/r^2. Note that for this simple source, the electric and magnetic fields are everywhere perpendicular to each other. As we will see, the current dipole is one of the most important concepts in biomagnetism, although magnetic dipoles are useful for interpreting the magnetic fields from magnetic materials in the body and also have been used to analyze the magnetocardiogram (MCG).

The calculation of the electric fields produced by current sources is a key problem in bioelectricity. By combining Ohm's law with the constraint that electric charge can neither be created nor destroyed, it is possible to show that the electric voltage V in the conductor obeys Laplace's equation, a general formula with analytical solutions for many situations. Since Laplace's equation has been well-studied by mathematicians, physicists, and engineers, there exists both an intuition and a mathematical tool kit that allows this equation and the voltage distribution it describes to be analyzed with comparative ease. A detailed knowledge of V can then be used to determine the electric current density $\vec{J}$ everywhere in the conductor.

Ampere's law, as we showed above, can be used to compute the magnetic field encircling the current source in Fig. 3c but, the net current enclosed by the imaginary curve c in Fig.

1a must now include the primary current I within the battery minus the return current $\vec{J}$ that would flow between the outside of the battery and c. This return current flows in a direction opposite to that of I and hence produces a magnetic field that partially cancels the field from the primary source I. There are several other ways to compute the magnetic field from the currents flowing in Fig. 3c. The law of Biot and Savart allows us to determine the magnetic field $\vec{B}(\vec{r})$ at the point $\vec{r}$. To do this, both the Ohmic current $\vec{J}$ returning through the saline and the primary current I within the battery and resistor are broken into small segments of current. The magnetic field produced by the entire current distribution is then computed by the vector addition of the contribution of each segment. Another approach uses a mathematical slight-of-hand to show that as long as the saline is homogeneous and has no boundaries, the summed contributions of $\vec{J}$ to $\vec{B}$ cancel themselves out, leaving only the magnetic field produced by I as it flows from the negative terminal, through the battery and resistor, and to the positive terminal. In this case, the current dipole alone appears to be the source of the magnetic field. While different mathematical operations are required in the three approaches, the results obtained are identical.

The problem of computing the magnetic field from electric current sources in conducting media is complicated by inhomogeneities. Suppose that the right-hand third of the saline bath in Fig. 3c has a conductivity that is substantially lower than that of the left-hand two-thirds. The lines of current density $\vec{J}$ would bend at the interface between these two regions, and this bending of current lines would alter the magnetic field, just as bending the wire in Fig. 1 into the loop in Fig. 2 changed the field. The actual calculation of how $\vec{J}$ is affected by the inhomogeneity can be a rather involved application of Laplace's equation, but this calculation is necessary before it is possible to determine $\vec{B}$. As always, the law of Biot and Savart can be used to compute the magnetic field $\vec{B}$ from the current density $\vec{J}$. Ampere's law is still valid, but because the symmetry of the original problem has been destroyed by the inhomogeneity, this law is of little practical value. A pedagogically-useful approach is to imagine that the saline bath remains homogeneous and extends to infinity in all directions, but that secondary current sources K are added to the bath at the locations that would correspond to the surfaces bounding the inhomogeneities. The strength of these secondary sources is adjusted to bend the current lines into the configuration that would exist in the inhomogeneous system. With this approach, the magnetic field is determined by the primary and secondary current sources and not by the Ohmic currents.

BIOLOGICAL CURRENT SOURCES

By now, we should have begun to develop an intuition regarding the relationship between electric currents and magnetic fields. In extending this discussion to examples that are more relevant to biology, we must address the problem of identifying a biological equivalent of Fig. 3b and 3c that does not utilize metal wires or electrodes or good, plastic insulators. We will first look at the current source and then turn to the necessary insulators and wires. Possibly one of the simplest sources of electric charge is a small glass sphere that is rubbed across a piece of silk so that the sphere has a net positive charge on its surface. When this sphere is in dry air (Fig. 4a), the electric field $\vec{E}$ points radially outward, just as does the hair on the head of a person who is touching the top of a high-voltage static electricity generator. This is consistent with Coulomb's law, which states that electric field lines start and stop on charges.

If we were to drop our glass sphere into a jar of electrically-conductive saline solution, the electric charge would no longer be trapped on the surface of the sphere, but could move away along the radial electric field lines, as shown in Fig. 4b. When viewed from far away, our charged sphere looks like a current monopole, i.e. a point source of current. If we modify Ohm's law to apply to continuous media rather than discrete circuit components, we find that the electric current density $\vec{J}$ equals the electric field $\vec{E}$ times the saline conductivity σ. Thus, we have radial lines of $\vec{J}$. Because of $\vec{J}$, the charge on the sphere decreases exponentially in time, so that 63% of the charge has left the sphere in an interval known as the "relaxation time." The relaxation time depends strongly upon whether the substance into

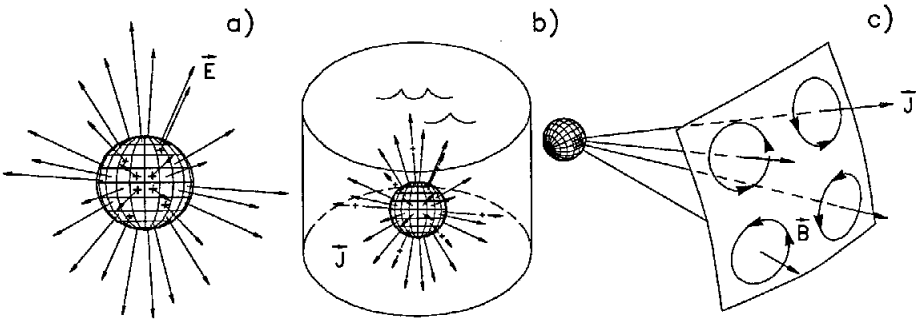

Figure 4. a) The electric field $\vec{E}$ produced by a positively-charged sphere in air. b) The electric current density $\vec{J}$ produced when the sphere in a) is immersed in saline to form a point current source. c) An illustration of how the magnetic fields $\vec{B}$ from the lines of current in b) cancel each other so that a point current source produces no magnetic field.

which the charge is placed is a conductor or an insulator. In quartz, an excellent insulator, the relaxation time is 9×10^5 s, while in copper, it is 1.5×10^{-19} s. Since the relaxation time for sea water is 2×10^{-10} s, the radial electric current produced when our charged sphere is dropped into saline will be significant for less than a billionth of a second. Because of this short time-scale, a charged object dropped into saline is not a good biological battery!

We can learn two other important points from the example in Fig. 4. First, if an object is made of saline or another reasonable conductor, free charges in such a system will distribute themselves throughout the system virtually instantaneously, at least on the time scale of the bioelectric signals we will consider. This type of argument provides the basis for the quasi-static approximation that is usually used in biomagnetic calculations. In this approximation, the bioelectric and biomagnetic fields at any instant in time can be viewed as being produced by the electric charges and currents extant at that same instant in time. Phase shifts, propagation delays, and the electric field induced by the time dependence of the biomagnetic field can all be safely ignored as long as the events considered are slow in comparison to the relaxation time. This in turn greatly simplifies the mathematics required to describe the electric and magnetic fields and their sources. As we will see later, the only significant exception to the quasi-static approximation that we need worry about relates to the electric fields across a nerve membrane, and this exception arises from the poor conductivity of nerve membrane and the ability of a nerve membrane to store electric charge. This should not be surprising when we consider that the duration of the nerve action potential and the relaxation time of nerve membrane are both about one millisecond.

Since the diffusion of electric charge through a conductor may be hard to envision, it is worthwhile to develop a simple analogy. Suppose that we pour a liter of water into a large, shallow tank. If we ignore any waves, we find that the water spreads out uniformly over the tank in a reasonably short time. Returning to our earlier definition of the quasi-static limit, we see that ignoring the waves is valid as long as we are interested in slow phenomena, such as the overall level of water in the tank. However, if we filled the tank with a dense plastic sponge, it would take much longer for the water to move to the far edges of the tank. Because the sponge has a capacity to hold water and the pores of the sponge delay the spread of the water, initially most of the water would remain close to the point where it was poured onto the sponge. Only with time would the water level in the tank reach equilibrium everywhere. Hence, external stimuli that disturb the water level in the tank might occur slowly enough to be treated as being quasi-static in a water-filled tank, but not in a water- and sponge-filled one. In most cases of interest to biomagnetism, the electrical properties of the human body are those of an oddly-shaped, saline-filled tank.

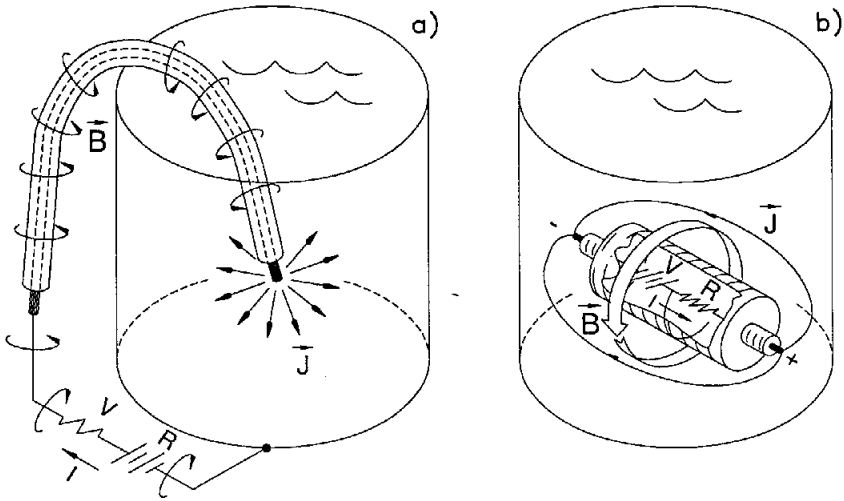

Figure 5. a) A point current source formed by the end of a wire immersed in a saline-filled metal bucket and connected to a battery. b) A self-contained current source consisting of two electrodes connected to a battery and a resistor, which are surrounded by a layer of insulation. The magnetic field, indicated by the broad arrow, encircles the source.

Our example of the charged sphere immersed in saline can also be used to demonstrate that a point source of current produces no magnetic field. Because of the spherical symmetry of the example in Fig. 4b, the current must flow radially away from our charged sphere, with the same current density in all directions. If we think of the current as flowing along the discrete lines shown in Fig. 4c, we realize that at a given distance from the source, each line of current must produce an equal magnetic field encircling the line, just as we saw in Fig. 1a. However, because each line of current has an identical line of current as a neighbor, the magnetic fields in the space between the two lines will be oppositely directed and will cancel each other out. It follows that everywhere outside the point current source the magnetic field is zero.

Our first attempt to create a biological battery was unsuccessful, so we will try another. Suppose we take an insulated wire, connect it to a battery and a resistor, and place one end in a metal bucket filled with saline, as shown in Fig. 5a. A wire connected to the bucket completes the electrical circuit, so that a steady current flows from the battery, through the resistor, along the wire, across the saline, and back to the battery. From the point of view of the electric fields in the bucket, the point current source formed by the end of the wire is almost identical to the spherical source of charge in Fig. 4. In this case, however, as charge flows away from the end of the wire and into the saline, this "lost" charge is immediately replaced by more charge provided by the battery, so that the electric field and current in the bucket do not decay quickly, but instead are steady. It is important to recognize that the spherically-symmetric current distribution outside the end of the wire produces no magnetic field, but the current flowing along the wire does. As we indicated before, when computing biomagnetic fields, it is important to include all of the electric currents that are flowing in the system. In the isolated sphere example, the stored charge had potential energy, which was dissipated as the charge flowed out into the saline. In the example in Fig. 5, electrical energy originating from the electrochemical processes within the battery is dissipated as the charge moves through both the resistor and the saline. As long as the battery is capable of providing this energy, the currents will flow. In our water analogy, in the steady state the surface of the water can be sloped only while water is being poured into the tank at one location and

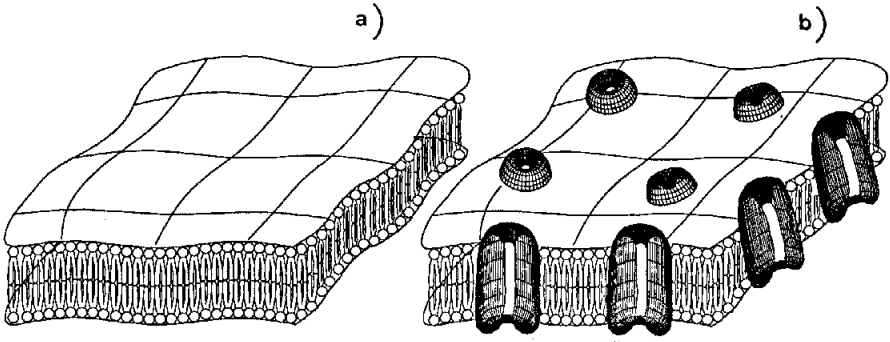

Figure 6. a) A schematic diagram of a segment of phospholipid membrane. Charged, hydrophilic head groups that are in contact with the water inside and outside the cell form the two surfaces of the membrane. Hydrophobic tails on the phospholipid molecules form the middle of the membrane and are responsible for the high electrical resistance of the membrane. b) The same membrane as a), but with ion-selective channel proteins spanning the membrane.

is drained out at another. The quasi-static limit is still valid as long as the current flow is either steady or changes slowly in comparison to the relaxation time.

The wire immersed in a bucket is not biologically realistic, but it suggests the key components for a biological battery: a source of electrical energy, and some form of an insulated conductor that allows the current to flow over a macroscopic distance without shorting itself out. Without insulation, positive and negative charges would cancel each other in the short relaxation time of less than a nanosecond. Figure 5b shows a simple system that is a reasonable approximation of many biological current sources: a voltage source, a current-limiting resistor, a layer of insulation, and a region from which current leaves the source and another at which it returns to the source. Just as in Fig. 3c, this current source looks like a current dipole whose field falls off as $1/r^3$ and has an encircling magnetic field that falls off as $1/r^2$.

In everyday life, insulating materials are made of plastic, ceramic, or glass, but none of these materials are available for constructing biological insulation. Figure 6 shows a phospholipid membrane that serves as the layer of insulation separating the inside and the outside of biological cells. The membrane is remarkably thin, less than one thousandth of the diameter of a typical nerve cell. While phospholipid is not a very good insulator in comparison to glass or quartz, it is sufficiently good that the membrane of a 1 mm long segment of 100 μm diameter nerve axon will have a resistance of 300 kilohms (kΩ), in which case a 70 mV potential difference across the membrane would result in a 0.2 μA current crossing that segment of membrane. As we will see later, the time-dependent voltages and currents in nerve and muscle cells arise not from the simple phospholipid membrane in Fig. 6a, but from the more complicated one in Fig. 6b in which the membrane is spanned by gating proteins that have time- and voltage-dependent conductances to specific ions.

THE RESTING MEMBRANE POTENTIAL

The cell membrane is a truly important component of a biological battery, since the relatively high electrical resistance of the membrane allows the inside of the cell to remain at a potential that is negative with respect to the outside. This can be observed experimentally, as illustrated in Fig. 7a. A microelectrode, made from a micropipette filled with a concentrated salt solution, can penetrate a cell membrane with minimal damage to the cell and thus can be used to measure the transmembrane potential, V_m. In typical nerve and muscle cells, V_m

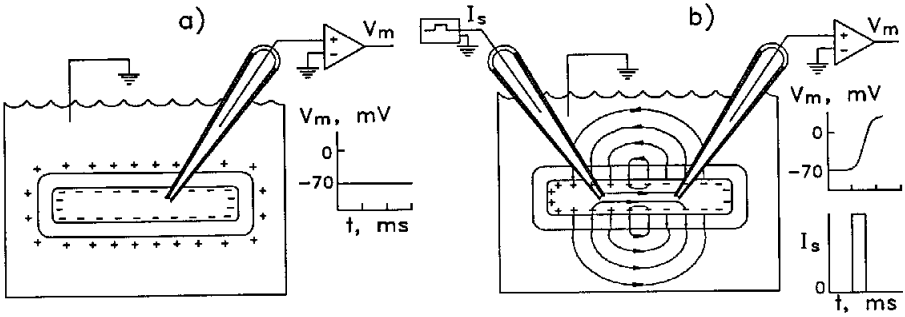

Figure 7. a) A measurement of the transmembrane resting potential using a glass microelectrode and a high-impedance amplifier. b) A measurement of an action potential initiated by an electrical stimulus I_s applied by a second microelectrode.

ranges from −70 to −90 mV. This potential difference means that there must be an excess of negative charge on the inside of the cell membrane, and an excess of positive charge on the outside. The positive and negative charges are dispersed uniformly over the outer and inner surfaces of the membrane, respectively, because like charges repel and opposite charges attract, and because charge is free to move through the relatively-good conductors formed by the intracellular and extracellular fluids, but not through the poorly-conducting membrane. Outside the resting cell, the electric fields from the two layers of charge cancel perfectly, as they do inside the cell, so that there is no electric field in either region. Within the membrane, however, the electric fields from the negative charge on the inner surface and the positive charge on the outer surface have the same magnitude and direction and hence add, producing an electric field of approximately 10^6 volts/meter inside the phospholipid. The capacity of the membrane to store electric charge arises from the fact that the opposite charges on the two surfaces of the membrane are held in place by this electric field.

A number of different mechanisms contribute to the resting transmembrane potential. Inside the cell, there is a high concentration of negatively-charged proteins that are too large to cross the membrane, but the corresponding positive counter-ions are free to cross the membrane and hence can exit the cell, leaving the inside of the cell slightly negative. Furthermore, the inside of a typical nerve or muscle cell has a high concentration of K^+ ions and a low concentration of Na^+ ions. The reverse is true for the extracellular fluid. As a result, there is a small but steady flux of Na^+ ions into the cell and of K^+ ions out. The cell must expend metabolic energy to operate a "sodium-potassium pump" that balances these ionic fluxes and maintains the cell in an electrochemical steady state. This pump in general moves 3 Na^+ ions out of the cell for every 2 K^+ that it moves into the cell, and as a result produces an electric current across the membrane that contributes to the negative transmembrane resting potential. The most important mechanism for producing V_m is the fact that the resting membrane is more permeable to some ions than to others. Each species of ion moves across the membrane at a rate that is determined both by the permeability of the membrane to the ion and by the net force on that ion. This force is the result of both the chemical concentration difference for that ion and the electric potential difference across the membrane. The steady state membrane potential occurs when all of the inward ionic currents are balanced by the outward currents. In the resting cell, the resistance of the membrane to K^+ ions (which tend to move outward) is typically 30 times smaller than to Na^+ ions (which tend to move inward). However, when V_m is at −70 mV, the net force on K^+ ions is one-thirtieth of the net force on Na^+, and as a result, the two ionic currents cancel and the cell potential remains constant in time. While there is a higher concentration of Cl^- outside of the nerve than inside, the electric potential difference across the membrane of the resting cell almost exactly balances this concentration difference, so that the chloride current is negligible at rest.

The resting membrane potential is stable against small disturbances. If a small amount of positive charge is added to the inside of a nerve cell, it will locally make the potential less negative. But this added charge will quickly diffuse away, so that in a millisecond or so, the originally-applied charge will move back across the membrane, thus allowing the membrane to return to its original potential everywhere. As a result of this, the small disturbance will be significant only within a few millimeters of the point where the charge is applied. While this passive response can be of the utmost importance in the short dendrites of the brain, it is not an acceptable method for moving information over the long distances of the peripheral nervous system. In our analogy, a drop of water applied to the surface of our sponge will not be felt very far away.

THE NERVE ACTION POTENTIAL

Although V_m is stable against small stimuli, larger ones produce a drastically-different effect. If an appropriate mechanical, chemical or electrical stimulus is applied to a nerve or muscle cell, it will induce a conformational change in the gating proteins that span the membrane, as in Fig. 6b. These proteins have an axial channel that will allow certain ions to pass through the protein (and hence across the membrane) when the protein is in one configuration but not when it is in another configuration. Earlier, we showed that the electric field in a resting membrane can be very strong; changes in this strong electric field can produce a conformational change in a gating protein. As shown in Fig. 7b, a second microelectrode can be connected to an electric pulse generator (i.e. a stimulator) so as to inject positive charge into the cell. For this example cell, when the stimulus raises V_m to –50 mV, which is above the stimulation threshold, the reduction in the membrane electric field triggers a conformational change in the sodium-channel protein, causing the permeability of the membrane to Na^+ to suddenly increase by two orders of magnitude. This results in a large influx of Na^+ ions, and V_m rises to +40 mV. That region of the cell is then termed "depolarized." In Fig. 7b, the inside of the cell is depolarized (positive) near the stimulating electrode, but is still negative at the opposite end. Because of the potential gradient along the axis of the cell, intracellular positive charge moves to the right, the transmembrane potential in the middle of the cell increases to –50 mV, and as a result the membrane in the middle of the cell becomes more permeable to Na^+. The right-ward flowing intracellular current continues, the region of high-sodium permeability also moves to the right, and eventually the right-most regions of the cell become positive. But here we see the fundamental aspects of the biological battery we have been searching for: when viewed from the outside, the outer surface of the cell is positive at the right end and negative on the left end. Inside the cell, electric current flows from left to right, and outside the cell, the current returns in the opposite direction. The inside and outside of the current source are separated by a layer of insulation. The similarity with Fig. 5b is perfect, except that for peripheral nerves, the current source moves along the nerve.

After a nerve cell has been stimulated, it is necessary to reset the transmembrane potential in preparation for a second stimulus, unless the animal you are constructing needs to "take only a single step." The cell is reset in two ways. First, the sudden increase in sodium permeability, which lasts for only a millisecond, is immediately followed by a decrease in sodium permeability. However, the inside of the depolarized cell still has an excess of positive charge, and decreasing the sodium permeability does little to reduce this. A transient increase in potassium permeability allows sufficient K^+ to leave the cell to return V_m to its resting value, or even to a slightly more negative value. The net effect of the depolarizing, inward Na^+ current and the repolarizing, outward K^+ current is to return the cell to its resting potential, but with a small chemical imbalance, which is subsequently corrected by the sodium-potassium pump.

THE PROPAGATING ACTION POTENTIAL

Figure 8 shows a rather simplified motor neuron as well as circuits that explain how the action potential propagates along the axon. The axon in Fig. 8a is a tube of phospholipid membrane filled with a saline medium, and thus serves as our insulated conductor. As we

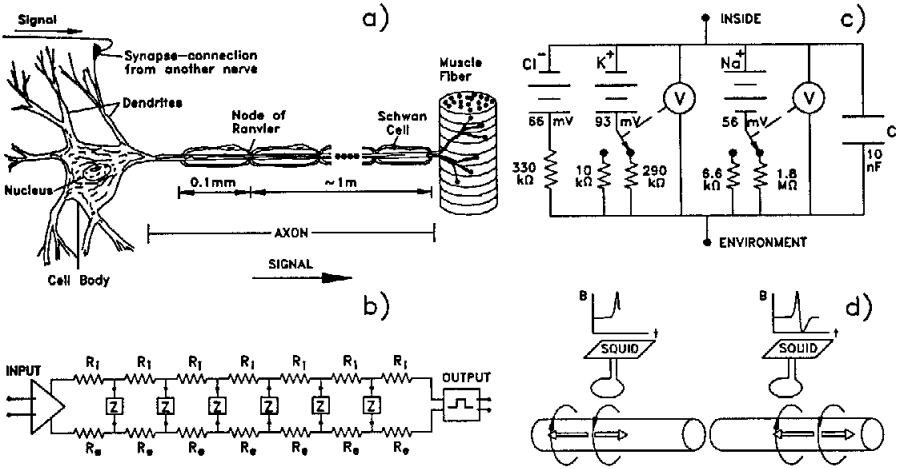

Figure 8. a) A motor neuron that connects a neuron from the brain to a muscle fiber. b) A schematic representation of a motor neuron, with the input amplifier connected to the output stimulator by an electrical cable consisting of an intracellular resistance R_i, an extracellular resistance R_e, and a membrane element Z. c) An overly-simplified circuit for Z that exhibits the voltage-dependent changes in sodium and potassium conductance associated with a nerve action potential. The values of the components correspond to a 1 mm by 1 mm patch of membrane. A more realistic model would replace each voltmeter, switch, and pair of resistors with a continuously-variable, time- and voltage-dependent resistor. d) The action current and magnetic field distributions that move along a nerve with a propagating nerve action potential. The magnetic field is measured with a Superconducting QUantum Interference Device (SQUID) magnetometer.

discussed earlier, because the resting membrane is leaky to potassium and chloride ions, a passive voltage would be conducted only a millimeter or two before being shorted out by the leakage pathway across the membrane provided by the membrane elements Z in Fig. 8b (shown in more detail in Fig. 8c). Hence, the propagation of signals over long nerves is dependent on the large sodium and potassium currents that are triggered by a stimulus, for example from another nerve. The voltage-controlled switches and resistors in Fig. 8c represent the variable ionic permeabilities discussed above; the batteries represent the chemical concentration gradients, and C represents the capacity of a segment of the membrane for storing electric charge. Extending our water analogy, the batteries correspond to the pressures in three different supply pipes that fill the tank from the bottom, and the resistance in series with each battery corresponds to a valve that limits the flow of water in each pipe. The capacitance corresponds to the size of the tank and thus its ability to store water. Depending upon the difference between the pressure at the bottom of the tank and the pressure in a particular pipe, water can flow through the valve in either direction, either raising or lowering the water level in the tank. When this level rises, so does the pressure at the bottom of the tank, and at some point the tank pressure will exceed the pressure in one or more of the pipes and the filling will slow and eventually stop. Opening one of the valves further will change the balance of flows between the pipes and the tank, until a new water level is reached. While it might not seem practical, it would be possible to propagate a water wave down a long tank by locally adding and then removing water from the tank by means of the successive opening and closing of valves distributed along the bottom of the tank. A nerve does just this by having ion channels distributed along its length, as shown by the boxes labeled Z in Fig. 8b.

Figure 8d shows how the depolarized region moves along the nerve, at a velocity of up to 120 m/s. It is important to recognize that the propagation velocity of a nerve is very

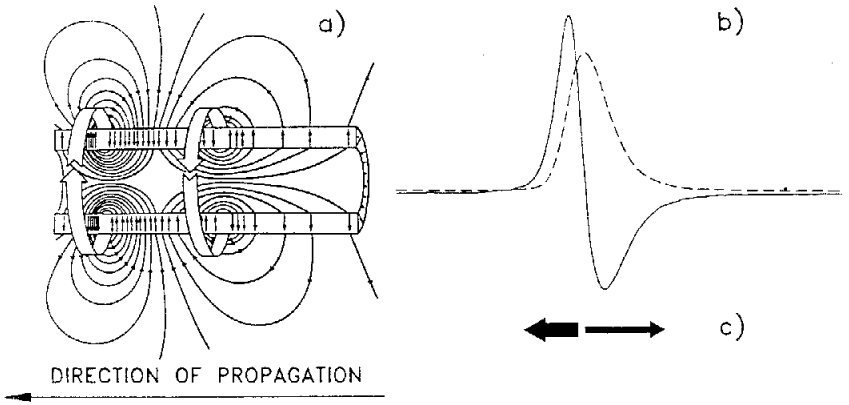

Figure 9. a) The electric current (thin arrows) and magnetic field (wide arrows) associated with a propagating nerve action potential. The thickness of the membrane is greatly exaggerated. b) The corresponding transmembrane potential (dashed) and the axial, intracellular action currents (solid). c) The depolarization (D) and repolarization (R) current dipoles consistent with a) and b).

much less than what one might expect from our earlier discussions of the quasi-static limit. In our discussion of Fig. 4b, we assumed that the conductivities were high and the capacitance (the ability of the material to store charge) was low. In situations involving cell membranes, neither of these conditions are met, and as a result, the quasi-static approximation does not apply within the membrane. This problem can be avoided, however, by treating the entire nerve as a time-dependent voltage source, just like the idealized source in Fig. 5b, in which case all electric and magnetic fields *outside of the source* are consistent with the quasi-static approximation. We already saw what adding the sponge did to our tank analogy; now try to imagine what would happen if we took a cylindrical sponge, wrapped it with a layer of plastic with small holes and many valves, and then immersed it in the tank!

BIOMAGNETIC FIELDS FROM NERVE AND MUSCLE

Now that we have described our biological battery, we need to show how this concept applies to the magnetic signals produced by various biological tissues. The electric and magnetic fields associated with the propagating nerve action potential are shown in Fig. 9a. Close to the nerve, Ampere's law indicates that the magnetic field is proportional to the intracellular action current. As a general rule, the waveform describing the axial, intracellular current closely resembles the time-derivative (i.e. the slope) of the transmembrane action potential waveform. Hence a monophasic (i.e. single polarity) action potential will produce a biphasic action current which can be detected by its biphasic magnetic field, as shown in Fig. 10a. The pair of opposing current dipoles in Fig. 9c is a good model for the source of the nerve action currents and fields. Since the magnetic field from a single current dipole decreases as $1/r^2$, it follows that the magnetic field from the opposing pair falls off as $1/r^3$. The transition from a $1/r$ fall-off close to the nerve to a $1/r^3$ fall-off far away is shown in Fig. 10b. The magnetoneurogram (MNG) from human peripheral nerves is difficult to detect from outside the body because of this rapid fall-off, even though such nerves are bundles of thousands of individual nerve fibers and carry total currents on the order of 1 μA.

Skeletal muscle fibers have electric and magnetic fields that are quite similar to those of peripheral nerve; but, since a single, small nerve fiber might activate 50 or more larger muscle fibers, muscle signals are much stronger. However, skeletal muscles have a graded response to stimuli that involves the recruitment and repeated firing of groups of fibers. While this generally results in good muscle control, it produces complicated time- and spatial-

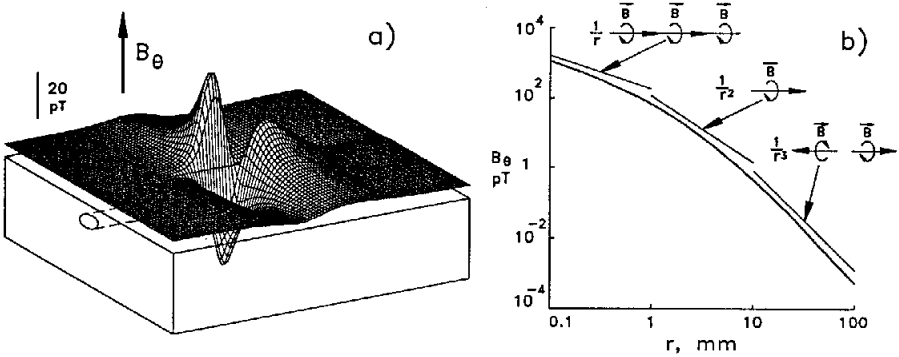

Figure 10. a) A theoretical prediction of the output of a magnetometer as it is scanned above an active nerve immersed in a conducting bath. b) A plot of the fall-off of the neuromagnetic field with distance from the nerve. Close to the surface of the nerve, the field falls off as $1/r$, as if it were produced by current in a long wire. Further away, the finite length of the depolarization or repolarization current causes the peak depolarization or repolarization field to fall off as $1/r^2$, as if the field were produced by a single current dipole. Even further away, both the depolarization and repolarization dipoles contribute to the field at the measurement point, and the field falls off as $1/r^3$, consistent with it being produced by an opposing pair of current dipoles.

dependences of the fields, which are recorded as the magnetomyogram (MMG).

The electric and magnetic fields produced by cardiac muscle are in some ways easier to understand than the fields from nerves and skeletal muscle. Unlike peripheral nerves, which are single cells of up to a meter in length, cardiac muscle is made up of a large number of individual cells, each on the order of 15 μm in diameter and 100 μm long. The intracellular spaces of adjacent cardiac cells are interconnected by a structure termed an "intercalated disk", which contains proteins that provide channels for the movement of ions between cells. Because of the electrical interconnections provided by these intercalated disks, cardiac tissue functions as if it was a syncytium, i.e. a single large cell. This is in contrast to skeletal muscle cells, which are not interconnected and can be stimulated individually. The electrical resistance of the intercalated disks results in the axial resistance of a strand of cardiac tissue being higher than that of a corresponding strand of peripheral nerve, and the propagation velocity is lower. As shown in Fig. 11a, the current and magnetic field distributions are similar to those of our original current source in Fig. 5b. However, the shape of the cardiac action potential in Fig. 11b is quite different from the nerve action potential in Fig. 9b, primarily because of a secondary inward current that brings Ca^{++} ions into the cell and maintains a long, depolarized plateau. Because the repolarization phase of the cardiac action potential is a hundred times longer than the depolarization phase, the repolarization currents are one-hundredth of the depolarization currents. As a result, the depolarization dipole is much more prominent than the repolarization one. For this reason and because of the large temporal and spatial separation of depolarization and repolarization, Fig. 11a shows only depolarization dipoles and a single loop of magnetic field. The single field maximum and the mirror-image minimum in Fig. 11c are characteristic of a single dipole current source, in contrast to the pair of current dipoles for peripheral nerve that result in the two maxima and two minima in Fig. 10a.

Our discussion of cardiac muscle has so far been limited to one-dimensional strands of tissue, such as the Purkinje fibers in the cardiac conduction system and the papillary muscle bundles within the ventricles. The vast majority of cardiac muscle, however, is a

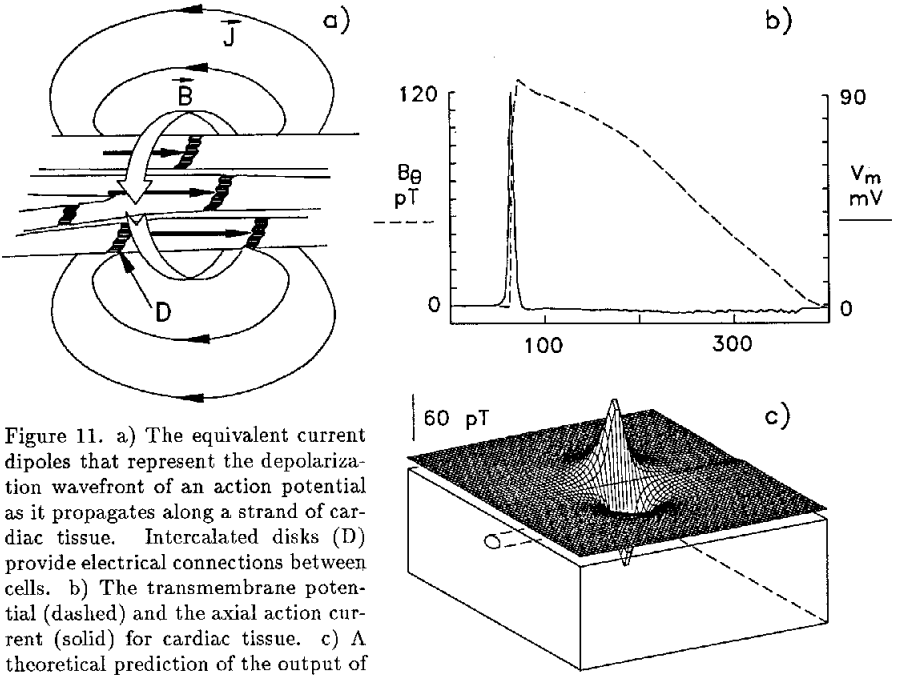

Figure 11. a) The equivalent current dipoles that represent the depolarization wavefront of an action potential as it propagates along a strand of cardiac tissue. Intercalated disks (D) provide electrical connections between cells. b) The transmembrane potential (dashed) and the axial action current (solid) for cardiac tissue. c) A theoretical prediction of the output of a magnetometer as it is scanned above an active cardiac fiber immersed in a conducting bath.

three-dimensional structure in which adjacent cells in all directions are interconnected. As a result, the depolarization wavefront in cardiac muscle is an extended surface, shown in Fig. 12a, that moves through the heart with a velocity of 1 m/s. The isolated current dipoles that we have used so far to describe our current sources are not appropriate in this case. It is better to divide the depolarization wavefront into many small segments, each of which has its own dipole. The magnetocardiogram (MCG) is determined by the sum of the magnetic fields of each segment of the wavefront. If we make the segments small enough, it is appropriate to think of the current dipole associated with each segment in terms of a current dipole density, termed the "impressed current" density $\vec{J}^i$, that is dispersed uniformly over the wavefront as is illustrated in Fig. 12b. It is worthwhile to note that it is theoretically possible for $\vec{J}^i$ to have an electrically-silent yet magnetically-detectable component that is tangential to the depolarization wavefront, but there have yet to be any conclusive experimental demonstrations that such sources exist in nature. If these sources occur, their anomalous fields may be most obvious close to the surface of the heart.

Calculations of the magnetic field from the distributed sources in the heart proceed with the same techniques we described before. We can use the law of Biot and Savart if we include the magnetic fields from both the primary, impressed current $\vec{J}^i$, and from the Ohmic return current $\vec{J}$. In cases of high symmetry, we can use Ampere's law. If the medium surrounding the heart is homogeneous, isotropic (the electrical properties are the same in all directions), and extends to infinity, then the contribution from $\vec{J}$ cancels out and only the magnetic field from $\vec{J}^i$ need be considered. In the inhomogeneous case, we can include secondary current sources $\vec{K}$ to account for the inhomogeneities.

The concepts we have presented so far can provide a rudimentary explanation of the magnetic fields of the brain, which are recorded as the magnetoencephalogram (MEG).

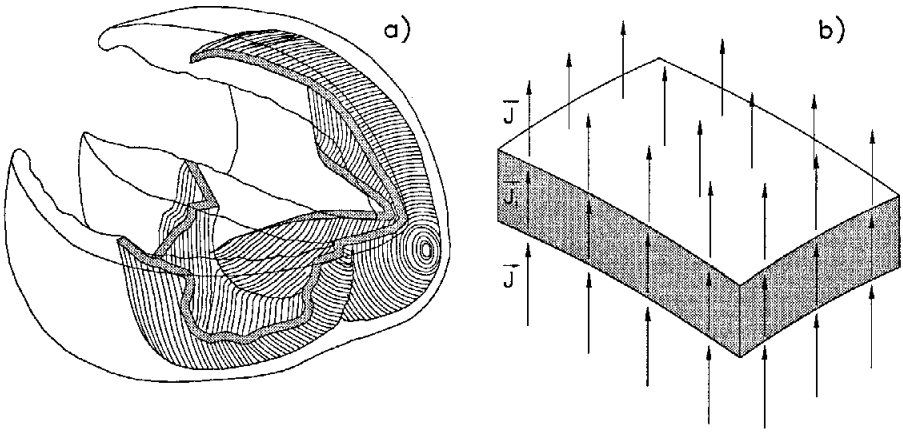

Figure 12. a) The depolarization wavefront propagating through the heart. The near chamber is the right ventricle and the far one is the left ventricle. (Adapted from a drawing by Ronald Selvester, personal communication). b) A representation of the current sources within a small segment of the wavefront in terms of an impressed current density $\vec{J}^i$, and the Ohmic current $\vec{J}$ that it produces.

Figure 13a shows a rather simplified view of the evoked field (EF) that is produced by the localized cortical response that immediately follows a sensory stimulus such as a pure tone applied to one ear, a flashing light seen by one eye, or an electrical stimulus applied to a finger. The magnetic field at an instant in time leaves the head at one location and reenters at another, with the actual locations depending on the specific stimulus used. If the field strength were plotted as a map, there would be a single, localized maximum, and a corresponding, symmetric minimum. Referring to our two-dipole source of a propagating nerve action potential (Figs. 9a and 10a) and the single-dipole source of a propagating cardiac action potential (Figs. 11a and 11d), we see that Fig. 13a suggests that the EF is produced by a single dipole. Observations so far of the time-evolution of MEG maps do not in general suggest propagation, but instead the data are consistent with the turning-on and turning-off of a stationary dipole, possibly followed by the energizing of another dipole. Electrical measurements suggest that the principal electrical activity arises from graded, post-synaptic potentials occurring in the dendrites of cortical neurons. While in the past it was believed that these dendrites behaved as simple, passive electrical cables, there is mounting evidence that dendrites too have ion-selective channels that control their electrical response to stimuli from connecting neurons. Of the different types of cortical neurons, those with dendritic networks that are spherically-symmetric about the cell body produce electric currents along the dendrites that have little or no external magnetic field, just as occurred in our example of the spherical current source. Only those neurons with dendrites that are centered about a point that is displaced from the cell body, such as in Fig. 13b, can result in a measurable current dipole moment with its characteristic field. If the synapses that are active in an evoked response are excitatory, the intradendritic space will become positive, and hence the cell body will be a source of positive current flowing into the adjacent tissue. If the synaptic input is inhibitory, the cell body will appear to be a current sink. Hence the sign of the dipole moment will depend upon the nature of the input, and could change during a response. Unfortunately, the magnetic field from a single cortical neuron is too weak to be detected outside the skull, and the evoked magnetic fields observed so far arise from the combined activity of 10^4 to 10^5 neurons, which are often in close proximity and appear to be functioning as a single unit.

So far, we have ignored the effects of the boundary of the conductor that contains the

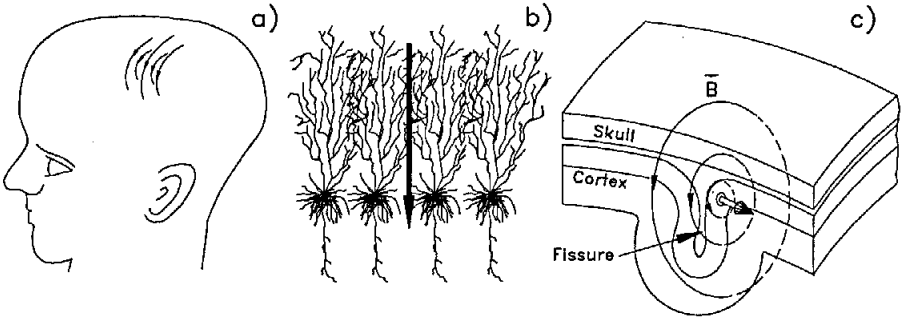

Figure 13. a) The magnetic field outside the skull from an evoked cortical response. b) The effective current dipole that describes the summed contributions of the dendritic activity of a population of simultaneously-activated cortical neurons. c) The relationship between the cortical dipole, the cortical fissures, and the evoked magnetic field.

current sources. For the MEG, the boundary formed by the skull has a profound effect, in that a radially-oriented current dipole will produce no external magnetic field. Hence the dipole that we detect with the MEG must be oriented tangential to the skull, and as a result the MEG arises primarily from cortical neurons located in the fissures, as shown in Fig. 13c.

Obviously most biological current sources are much more complex than the simple ones we have just described; but, the principles that govern their electric and magnetic fields are the same as those we have outlined. We can now shift our attention to the harder problem of obtaining a description of the biological sources given measurements of their fields.

THE INVERSE PROBLEM AND MODELLING

Early in our discussion, we described how to calculate a magnetic field from a knowledge of the currents that produced it. We start with a detailed description of both the geometry and the electrical conductivity of the region that has current flowing in it. Given the source distribution $\vec{J}^i(\vec{r}')$, where $\vec{r}'$ specifies the locus of points that spans the conducting region, we can use Laplace's equation and Ohm's law to calculate $V(\vec{r}')$ and $\vec{J}(\vec{r}')$ everywhere in the conductor. We then use the law of Biot and Savart to calculate $\vec{B}(\vec{r})$, where $\vec{r}$ corresponds to the location where we want to know the fields. Such calculations constitute solutions to the "forward problem." Ideally, it would be as straightforward to solve the "inverse problem" of determining exactly what sources, i.e. what $\vec{J}^i(\vec{r}')$, produced a measured magnetic field $\vec{B}(\vec{r})$ or electric potential $V(\vec{r})$, but in fact it is not.

There are many different techniques that can be used in solving the inverse problem. The most common is the least-squares approach that starts with an initial guess as to the source distribution, computes the field that this source would produce, compares the mean-squared error between the observed and calculated fields, and then adjusts the source to minimize this error. This process is repeated until the solution converges on a single set of source parameters, or until the investigator gives up. Unfortunately, it is an undisputable consequence of Laplace's equation that, in general, the three-dimensional inverse problem has no unique solution. Many, or even an infinite number of solutions, could produce the same external fields. While mathematical, physical, physiological, and/or metabolic constraints may eliminate certain solutions and guarantee a stable, repeatable calculation, there is always the justifiable concern that the sources that are estimated to have produced the observed fields may have little resemblance to the actual physiology.

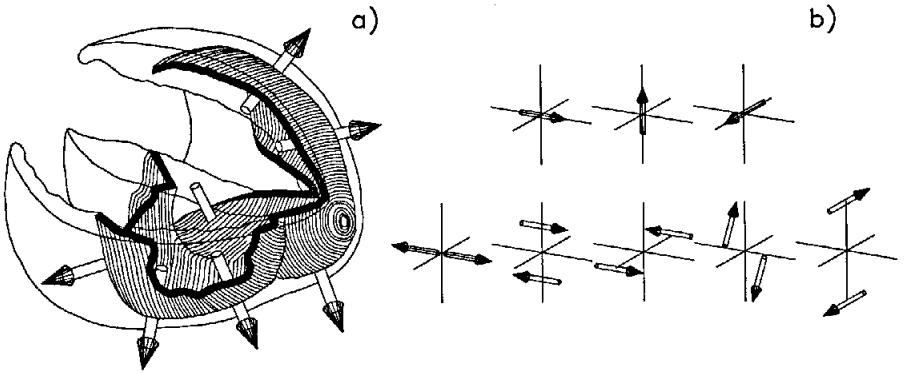

Figure 14. a) A multiple-dipole model for a cardiac activation wavefront. b) A pictorial representation of the first 8 terms of a multipolar current source model.

Based upon this caveat regarding the lack of a unique solution to the inverse problem, it is reasonable to ask what can be learned from either electric or magnetic measurements. If the exact nature of the current source is well known, for example a simple current dipole, then the time-dependent location, strength, and orientation of the dipole can be determined. If the source is more complex, it is necessary to use a more complex model. Fields from action potentials propagating along a nerve require a pair of dipoles. Since the cardiac wavefront in Fig. 12a resembles a sheet of current sources, one might model it as a large number of current dipoles, each of which accounts for the contribution of a portion of the wavefront, as shown in Fig. 14a. However at this level of complexity, problems of stability, uniqueness and noise often set in. While such a model may produce valid results when used for a forward calculation, it may not produce the expected result when used in an inverse one. The modeler is often tempted to use a mathematically-elegant but physiologically-unrealistic solution that consists of a multipole series such as that in Fig. 14b. The first three terms of the multipole series are simply three current dipoles with perpendicular orientations. The next five terms are the quadrupoles, which can be thought of as being constructed from pairs of dipoles. Octapoles and hexadecapoles follow. Mathematically, each of these sources would be superimposed at a single point and their strengths would be adjusted to best fit the observed field. This approach is productive if the primary goal is to obtain a compact mathematical description of the fields, but may provide little insight into the physiology or pathology of the biological sources. Overall, the safest approach to modeling is to first master the forward calculation that provides the desired level of physiological detail without becoming mathematically intractable, and then to use this model as the starting point for an inverse calculation. The modeler must recognize the possibility that constraints may have to be added to the inverse model, for example to prevent the individual cardiac dipoles in Fig. 14a from pointing in the wrong direction.

THE FUTURE

The lack of a unique solution to the inverse problem plagues bioelectric and biomagnetic measurements alike, and thus biomagnetism should not be thought of as the panacea for the limitations of bioelectric techniques. Instead, the enthusiasm for biomagnetism arises from a number of situations where fundamental or practical differences between the two techniques can be exploited. For example, a radial cortical current dipole will have a simple electric pattern but no external magnetic field, while a tangential dipole will have a clear magnetic signature. Thus the MEG is good for studying activity located in a cortical fissure.

Biomagnetic fields are influenced less strongly by intervening tissue, such as the skull, than are bioelectric fields and for this reason magnetic localization of bioelectric current sources may prove to be mathematically easier, more accurate, and/or more convenient than electrical localization. The MEG does not require a reference electrode, as does the EEG. As the number of magnetometers in multichannel SQUID systems is increased, it will become easier to map the MEG than to prepare and apply a large number of scalp electrodes. Biomagnetic fields are more closely related to intracellular currents than are extracellular potentials and thus, magnetic measurements on single nerve or muscle fibers readily allow determination of the transmembrane action potential without penetration of the cell membrane. It is easier to detect steady electric currents flowing within a person or animal by detecting the associated magnetic field than by recording surface electric potentials at the skin.

Fundamental differences between electric and magnetic fields may also exist. For example, we should now recognize that magnetic fields provide information about currents while electric measurements provide information about voltage. But current and voltage are related by Ohm's law to the resistance. In systems such as the heart, the complexity and importance of the electrical resistance of anisotropic tissue is acknowledged but poorly understood. There is reason to believe that biomagnetic recordings may help explain several confusing aspects of the propagation of cardiac activity. There may even exist physiological current sources that are magnetically-detectable yet electrically-silent, but these have yet to be found.

Thus, for either practical or fundamental reasons, biomagnetic measurements may provide solutions to problems in clinical medicine or basic science. Perhaps even more exciting applications of this new technology are awaiting discovery. In any case, the critical evaluation of emerging biomagnetic techniques will require a balanced and thoughtful comparison of both the measurement of electric and magnetic fields and the modeling of their sources.

ACKNOWLEDGEMENTS

The preparation of this manuscript has been supported by National Institutes of Health Grants NS 19794 and NS 24751 and by the College of Arts and Science of Vanderbilt University. I am indebted to Licheng Li for the skill and care with which she prepared illustrations. I thank John Barach, Richard Friedman, Nestor Sepulveda, Carlos Trenary, Ranjith Wijesinghe, and Leonora Wikswo for their comments on the manuscript, and Sam Williamson for his encouragement and patience.

REFERENCES

Hobbie, R.K., 1988, "Intermediate Physics for Medicine and Biology," Wiley, New York.

Kuffler, S.W., Nichols, J.G., and Martin, A.R., 1984, "From Neuron to Brain," Sinauer, Sunderland, Massachusetts.

Macfarlane, P.W., and Lawrie, T.D.V, (Editors), 1989, "Comprehensive Electrocardiology: Theory and Practice in Health and Disease," Pergamon Press, New York.

Wikswo, J.P., Jr., Malmivuo, J. A. V., Barry, W.H., Leifer, M.C., and Fairbank, W.M., 1979, Theory and Application of Magnetocardiography, in: "Cardiovascular Physics", D.N. Ghista, E. Van Vollenhoven and W. Yang, Eds., Karger, Basil, pp.1-67.

Williamson, S. J., Romani, G.-L., Kaufman, L., and Modena, I., (Editors), 1983, "Biomagnetism, An Interdisciplinary Approach," Plenum, New York.